J. Fluid Mech. (1966), *vol.* 26, *part* 1, *pp.* 1–15
Printed in Great Britain

The peeling of a flexible strip attached by a viscous adhesive

By A. D. McEWAN AND G. I. TAYLOR
Cavendish Laboratory, Cambridge

(Received 26 November 1965)

The peeling of a flexible strip from a rigid surface to which it is attached by a thin layer of adhesive is discussed, treating the adhesive as a Newtonian viscous fluid. This makes it possible to examine the flow and stress distributions ahead of the point where separation occurs. The conditions at this point are taken to be the same as those observed in other cases where a stream of viscous fluid separates into two. In particular, the effect of surface tension at the separating meniscus on the speed of peeling is predicted.

Experiments are described in which a sheet of 'Melanex' 4 μm thick was laid on a sheet of fluid covering a piece of plate glass. The apparatus was designed to ensure that this was peeled off at a constant angle, and the speed of the separation meniscus, as well as the load on the sheet, was measured. The experimental results are analysed in the light of the theory and shown to be consistent with it.

An interesting feature is the prediction that at low peeling speeds there is a great reduction in the thickness of the adhesive layer immediately ahead of the line of separation. Although the initial thickness of the layer dictates the scale of the shape adopted by the strip ahead of this line, it exerts no effect upon the relation between the external variables.

It is noted that, when the adhesive layer remains intact ahead of separation, the physical appearance of commercially available tapes in slow peeling can resemble that of simple viscous adhesives.

1. Introduction

When a flexible sheet is peeled from a rigid surface to which it has been attached by a layer of adhesive, the stress within the adhesive resisting the peeling is confined to a region near to the line of separation or rupture. Such a situation commonly arises in the stripping of what are technically known as 'pressure-sensitive' adhesive tapes. In this application, numerous experimental studies have been made of peeling adhesion, but a satisfactory rationalization of the observed behaviour is impeded by the difficulty in taking full account of the complicated rheological properties which most good adhesives are known to possess.

A simplification that has been the basis of several theoretical models is the assumption of purely Hookean elastic adhesive properties, with each connecting adhesive element acting independently of its neighbours and with failure occurring when a limiting stress condition is reached (e.g. Bikermann 1957; Kaelble

1960). With such a model, the strain energy in the adhesive when it fails (W) is related to its breaking strength and its elastic properties in such a way that W could be determined by appropriate experiments using other means than peeling a strip from a rigid surface. In this model, the tension T needed to peel unit width of strip when applied at an angle θ to the rigid surface is directly connected with W through the equation

$$W = T(1-\cos\theta), \tag{1}$$

so that T could be calculated using values of W determined independently.

However, models assuming elastic deformation to failure cannot account for the observation that many adhesives peel at a rate which depends upon T. Then although (1) remains true it is of less value in relating T with θ. These quantities might still be connected using approximations to the visco-elastic properties of the adhesive (e.g. Chang 1960) determined perhaps by simple tension-extension-time experiments but it is questionable whether the distribution of stress, strain and rate of strain within much of the critical region would be same as that in a simple one-dimensional experiment.

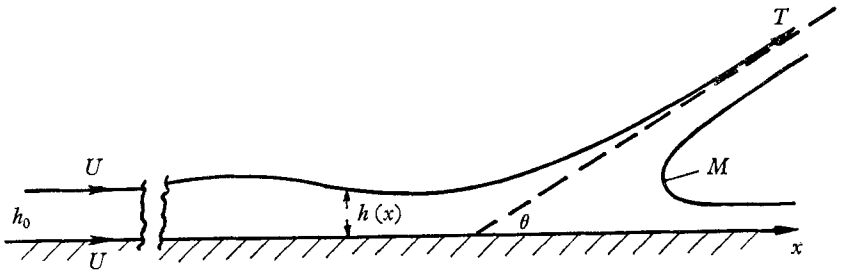

FIGURE 1. Peeling model.

For some adhesives, the rate of propagation U of the separation region is nearly proportional to T over a considerable range of values of T. For such cases, (1) shows that W is proportional to U. This is characteristic of Newtonian viscosity.

It is perhaps surprising that few theories of peeling have been proposed on the assumption that the adhesive possesses no elastic strength and is purely viscous. This neglect is probably due, in part, to the difficulty of defining suitable criteria for finding the position of the line of separation or rupture in an adhesive layer between diverging surfaces, if no specific 'failure' condition can be given.

In this note, use is made of the similarity between the separation of a viscous layer in the present context, and the previously studied cases in which a liquid layer confined within a narrow space between rigid boundaries is forced to divide about an advancing free surface, to enable the rupture position to be defined and a full description found. The model considered is a completely flexible sheet separated from a plane rigid surface by a Newtonian liquid layer of viscosity μ and initial thickness h_0. Reference is made to figure 1. The co-ordinate system is fixed with respect to the moving tear by imposing the propagation velocity U. The motion is taken to be steady and two-dimensional. When the liquid separates, part of it adheres to

the surface and part to the sheet. The total amount per unit area adhering to both surfaces is equal to that far upstream of the separation point, but the amount of fluid occupying the diverging space immediately before the separating meniscus M must depend upon how easily it is able to flow in the region of this space.

We confine our attention to small peeling angles θ, for which the Reynolds approximations greatly simplify the analysis; furthermore, we assume that the Reynolds number $\rho U h_0/\mu$ is negligibly small in cases of practical interest. Then the depth of the fluid h at position x will depend upon μ, and the longitudinal pressure gradient dp/dx is related to h by

$$(h-h_0)\,U = (h^3/12\mu)\,dp/dx, \tag{2}$$

p being the pressure excess over the atmospheric pressure. When the strip is inextensible but possesses no flexural rigidity, then, for small slopes,

$$T\,d^2h/dx^2 = -p. \tag{3}$$

Combining equation (2) and the derivative of equation (3),

$$\frac{d}{dx}\left(\frac{T\,d^2h}{dx^2}\right) = -12\mu U\left(\frac{h-h_0}{h^3}\right). \tag{4}$$

The x-wise variation in T is given approximately by

$$T/T_0\left(\cos\phi + h\frac{d\phi}{dx}\right) = 0, \tag{5}$$

where T_0 is the tension at points where the local slope ϕ of the strip is zero, and internal pressure is $-T\,d\phi/dx$. Since ϕ is always small, however, the tension T can be taken as constant, and, with new variables $\zeta = h/h_0$, $\xi = x\alpha^{-\frac{1}{3}}/h_0$, $\alpha = T/12\mu U$, equation (4) becomes

$$\zeta''' = (1-\zeta)/\zeta^3, \tag{6}$$

which is valid when $\alpha^{-\frac{1}{3}}\zeta' = \tan\phi$ is small. Primes denote differentiation with respect to ξ.

The initial boundary condition for all solutions of interest in the present case is $\zeta \to 1$ as $\xi \to -\infty$, and in the vicinity of $\zeta = 1$ the equation is approximated by

$$\zeta''' = 1-\zeta. \tag{7}$$

For which the solution is

$$\zeta - 1 = A e^{-\xi} + B e^{\frac{1}{2}\xi}\sin\left(\tfrac{1}{2}\sqrt{3}\xi + \epsilon\right). \tag{8}$$

A must be taken as zero to ensure that as $\xi \to -\infty$ the fluid is stationary with respect to the bounding surfaces. Thus

$$\zeta' = \zeta'' = \tfrac{1}{2}B\sqrt{3} \quad \text{as} \quad \zeta \to 1. \tag{9}$$

This provides a convenient starting-point for the numerical integration of equation (6). For reasons explained later it is necessary to obtain a set of solutions represented by different values of B. Since $(\zeta-1)$ is periodic, with period $4\pi/\sqrt{3} = 7{\cdot}26$, solutions which start with a given value of B are repeated when B increases in ratio $e^{2\pi\sqrt{3}} = 37{\cdot}622$ times. This provides a convenient check as to whether any particular choice of B is small enough to warrant the use of equations (8) and (9) for initial values in the numerical solution of equation (6).

1.1. *Physical conditions at the meniscus*

The physical conditions at the meniscus are unknown but there is no reason to suppose that they differ from those at the meniscus between rigid diverging surfaces. The case bearing the closest similarity to the present one would be that in which the rigid surfaces each travelled at the same velocity with respect to the minimum gap position. Experiments have been performed by Pitts & Greiller (1961) in which two partly immersed rollers were driven in opposite directions of rotation. The liquid drawn through the narrow gap between the rollers formed a meniscus ahead of this gap, the position of which could be measured. Unfortunately, the data are of limited extent and it is necessary to consider the analogous case dealt with by Taylor (1963) of motion in which one surface is fixed and the other moves away from the meniscus. Such motion arises in a partly filled journal bearing. Taylor pointed out that two conditions must be fulfilled at the meniscus and that they both depend upon $\mu U/\sigma$, where σ is the surface tension. The conditions are: (i) that for determining the pressure drop† between the atmosphere and some point upstream of the meniscus in the liquid; and (ii) that which gives m, the ratio of the thickness of the layers of fluid adhering to the moving surface (surfaces) to the width of the gap at the meniscus.

The experimental determination of these conditions as a function of $\mu U/\sigma$ is a matter of some difficulty. No measurements have yet been made of pressure drop across the meniscus (condition (i)), for either case. For the second condition, results were obtained in both the above-mentioned studies. However, a complication arises in the definition of m from these results. The value of m can be found simply by determining both the meniscus position (which defines h_m, the width of the gap at the meniscus) and the amount of liquid adhering to the moving surfaces after passing the meniscus. This method was used by Pitts & Greiller in an attempt to find $\lambda = q/Uh_0$, a parameter defining the amount of liquid passing through h_0, the maximum gap width upstream of the meniscus. Here q is the volume flux per unit width, and U is the surface velocity. Since the determination of q was insensitive they confine their published experimental results to measured values of h_0/h_m. λ is a number which depends upon the geometry of the surfaces and the fluid conditions on both sides of the nip h_0, but, if λ could be defined, then m would be given as

$$m = \lambda h_0/h_m. \tag{10}$$

The value of λ, when both sides of the nip are flooded, is $\frac{4}{3}$. If h_m is substantially larger than h_0 the effect of the meniscus in altering the value of λ should be small.

Adopting this value for λ, the results given in figure 3 of Pitts & Greiller's paper, together with some extra data kindly supplied by Dr Pitts, were used to prepare figure 2. The results are seen to lie fairly close to the line $m = 0{\cdot}63(\mu U/\sigma)^{\frac{1}{2}}$ but the exponent of the curve of best fit seems to be slightly lower. Although there is no theoretical reason for supposing that the points asymptotically approach

† The quantity here described as 'pressure drop' and represented later by the symbol δp in equation (13) is the difference between the pressure in the air outside the meniscus and the pressure which would exist according to Reynolds approximation if the flow had continued undisturbed up to the position of the meniscus (see Taylor 1963).

a parabolic form for low $\mu U/\sigma$, this form occurs in two other analogous situations, namely in the driving of a viscous liquid from a cylindrical tube by a long bubble† (Fairbrother & Stubbs 1935; Taylor 1961; and in the journal-bearing case of Taylor 1963). In each case the multiplicative factor is different, as might be expected from the different physical configurations. A second characteristic common to these analogous situations is that the value of m apparently approaches asymptotically a value less than 1 as $\mu U/\sigma$ becomes large (Taylor 1961;

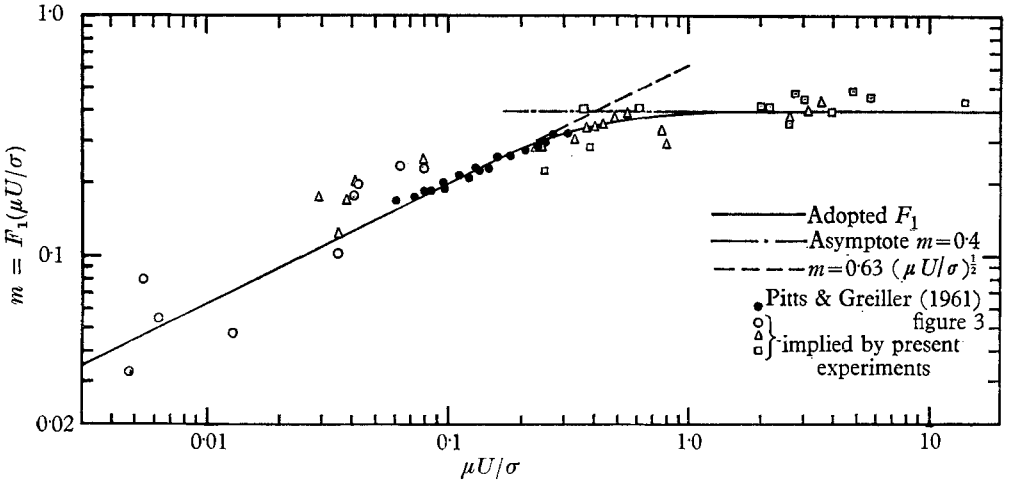

FIGURE 2. $m = 1/\zeta = F_1(\mu U/\sigma)$ as a function of $\mu U/\sigma$.

Cox 1962; Taylor 1963) and, from the appearance of Pitts & Greiller's results on figure 2, such levelling off of m may also be occurring in their experiments using two rollers. There is no direct experimental evidence which would enable us to give an exact value for m_∞, the asymptotic limit of m, and for the analysis it was assumed to be 0·4. Subsequent experimental results, given later, confirmed that this assumption was reasonably accurate.

1.2. *Application of meniscus conditions to the peeling-strip solution*

Details of the solutions of equation (6) describing the gap width as a function of position are given in the next subsection. It is useful to consider first what information is required from these solutions.

Far upstream of the meniscus, the liquid film is undisturbed and is stationary with respect to the plane and the strip, occupying a gap of width h_0. For this case therefore, $\lambda = 1$ and m is simply

$$m = h_0/h_m = \zeta_m^{-1}. \tag{11}$$

In this case we assume that with small peeling angles

$$m = F_1(\mu U/\sigma). \tag{12}$$

† Bretherton (1961) theoretically predicts a $(\mu U/\sigma)^{\frac{2}{3}}$ relationship at very low driving speeds, but his experimental results are inclined to suggest a somewhat lower exponent.

In the complete absence of data on the pressure drop through the meniscus one can only speculate upon its probable magnitude, but dimensional analysis suggests that its form is

$$-\delta p = \frac{\mu U}{h_0 \zeta} F_2\left(\frac{\mu U}{\sigma}\right). \tag{13}$$

When $\mu U/\sigma$ is very small, surface tension will dominate and the pressure drop will be approximately

$$-\delta p = 2\sigma/(h_0\zeta),$$

so that

$$F_2(\mu U/\sigma) = 2\sigma/(\mu U). \tag{14}$$

For $\mu U/\sigma$ large, the shape of the meniscus approaches one defined by viscous stress alone and dimensional arguments suggest that

$$-\delta p = C\mu U/h_0\zeta,$$

where C is a constant, almost certainly positive and probably less than 1·0. Thus, when $\mu U/\sigma$ is large, the change in pressure across the meniscus is of the same order as that occurring over an x-wise distance of h_0.

Immediately ahead of the meniscus the pressure condition, using equation (3) and the terms defined before equation (6), is

$$\alpha^{-\frac{2}{3}} T/h_0 = -\delta p, \tag{15}$$

or

$$\zeta'' = \tfrac{1}{12}\alpha^{-\frac{1}{3}} F_1 F_2. \tag{16}$$

Since the slope of the strip does not change after the meniscus,

$$[\zeta']_{\zeta=m} = \alpha^{\frac{1}{3}} \tan\theta. \tag{17}$$

Thus, the end boundary conditions describing the shape of the strip rely upon a knowledge of F_1 and F_2. For F_1, the solid line of figure 2 is taken, but for F_2 equation (14) can only be justifiably adopted for low values of $\mu U/\sigma$.

From equations (11), (16) and (17) the solution of equation (6) is related to the externally measurable quantities in a peeling experiment, namely $\mu U/\sigma$, α and θ. Solutions of the equation must therefore yield the functional relationship between ζ, $d\zeta/d\xi$ and $d^2\zeta/d\xi^2$. The value of ξ is immaterial.

1.3. *Solutions of equation* (6) *and their conversion to a usable form*

Equation (6) was solved by numerical integration using the Cambridge University Mathematical Laboratory's 'Edsac II' digital computer. A Runge–Kutta method was adopted, and the interval of integration was made variable depending upon the value $d^2\zeta/d\xi^2$ in order that accuracy could be retained when quantities were varying rapidly. A test of accuracy could be obtained by performing the integration with various basic step sizes.

Integration was commenced from $\zeta = 1$ with ζ' and ζ'' equal according to equation (9) and with values of B between $8{\cdot}66 \times 10^{-5}$ and $2{\cdot}60 \times 10^{-3}$ chosen from trial solutions performed by Dr R. Herczynsky, to cover adequately the resultant range of variables. Some representative results are presented in figure 3. The pattern of results repeats itself in ξ with a period of $4\pi/\sqrt{3}$. Integration was commenced from $\xi = 0$, but for all initial values of ζ' and ζ'' covered by the calculations the variation in ζ is insignificant before $\xi = 6$. It will be seen that for all

initial values ζ undergoes one or two cycles of oscillation of rapidly increasing amplitude before depearting monotonically from the ξ-axis. The number of cycles of oscillation before departure is fixed by the initial values of ζ' and ζ'', but it can be demonstrated that all solutions must finally approach infinity.

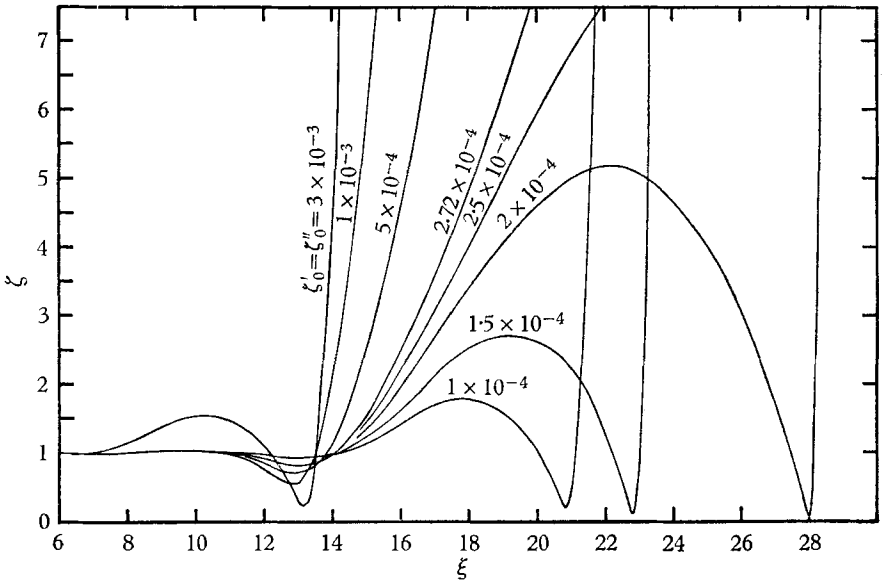

FIGURE 3. Dimensionless form of peeling strip.

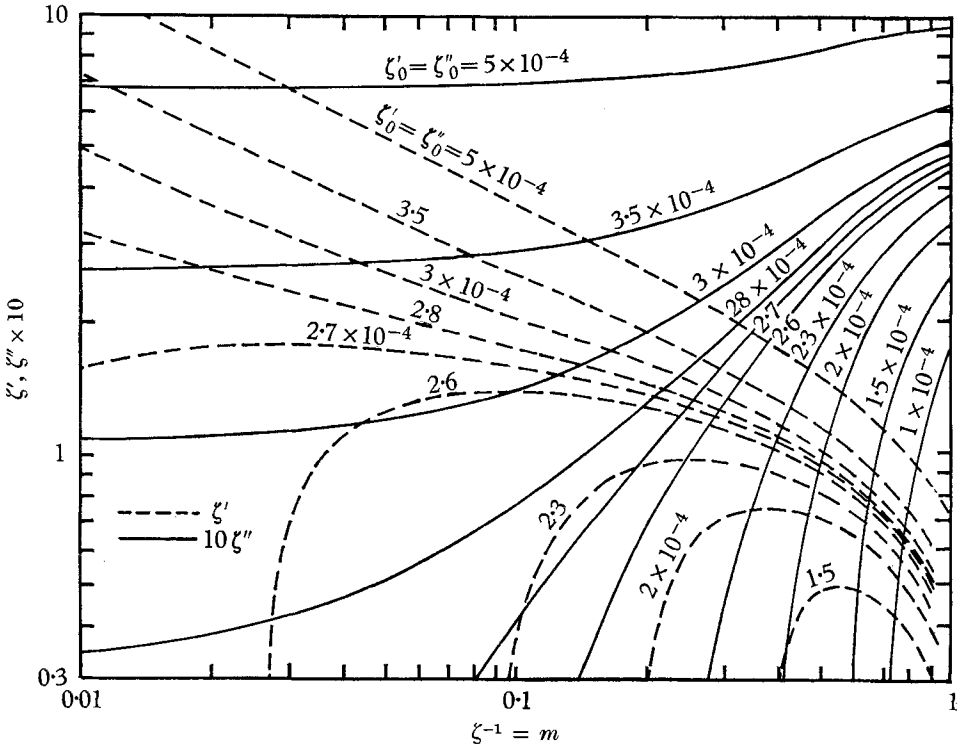

FIGURE 4. ζ' and ζ'' vs. $1/\zeta$.

There seems to be no analytical way of finding the initial conditions for monotonic departure in a given cycle. This occurs in the nth cycle, where n is the least integer for which $B > (37{\cdot}622)^{-n}B_0$, and B_0, determined from computer solutions of (6), lies between $2{\cdot}365 \times 10^{-4}$ and $2{\cdot}375 \times 10^{-4}$. Below the latter value, ζ will execute a further half cycle before departure, and in this case the minimum value of ζ after this half cycle varies inversely with its amplitude, and the gradient of departure is subsequently steeper. Figure 4 plots ζ' and ζ'' as a function of ζ for those parts of the curves of figure 3 which exhibit positive values of these derivatives. The abscissa is written, for convenience, ζ^{-1}, which by equation (11) corresponds to m.

From figure 4 a plot of ζ' against ζ'' can be made for constant values of m. Now, by equation (16), ζ'' is given as a function of F_1F_2 for constant values of α.

m	Appropriate $\mu U/\sigma$	Selected $\mu U/T$	Corresponding ζ''	ζ'	$\theta°$
0·3	0·249	10^{-2}	0·0992	1·075	28·0
		10^{-3}	0·0459	0·969	14·0
		10^{-4}	0·0214	0·917	5·58
		10^{-5}	0·00992	0·892	2·53
		10^{-6}	0·00460	0·880	1·157
		10^{-7}	0·00212	0·874	0·532

TABLE 1

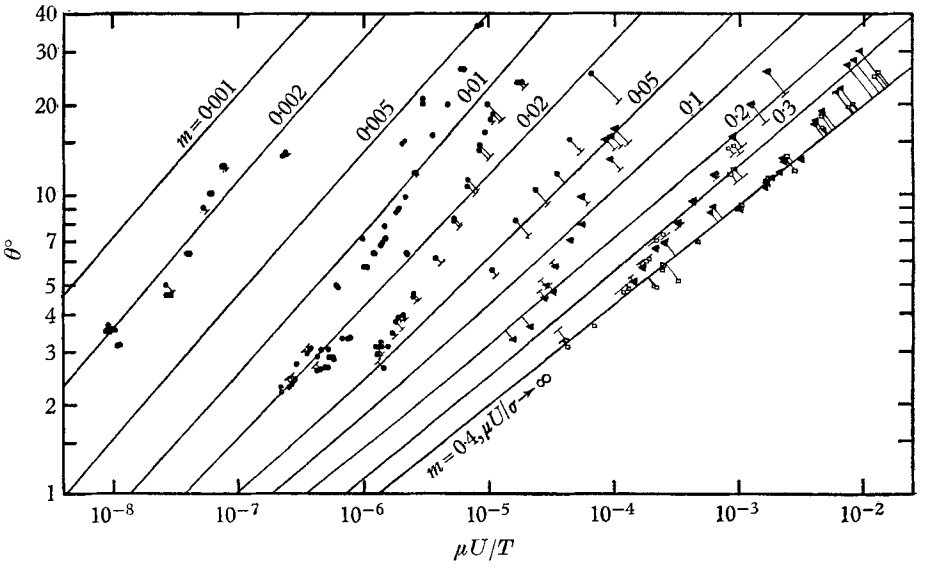

FIGURE 5. $\mu U/T$ as a function of θ; theory and experiment. The flags on symbols represent the comparison between theory and experiment. The line at the base of the flag marks the m curve upon which the point should lie if figure 2 were correct. For points without flags the curve coincides to within the symbol radius. ●, Ethyl alcohol; ▲, castor oil; □, Limea Oil.

Since F_1 and F_2 have been taken as functionally related to $\mu U/\sigma$ with values given by figure 2 and equation (14), respectively, ζ'' can be expressed in terms of m, $\mu U/\sigma$ and α:

$$\zeta'' = m(\mu U/\sigma)\sigma/6\alpha^{\frac{1}{3}}\mu U, \tag{18}$$

which enables m, α and θ to be related. As a typical calculation, take $m = 0{\cdot}3$, $\zeta = 3{\cdot}333$ and, from figure 2, $\mu U/\sigma = 0{\cdot}249$. Try $\frac{1}{12}\alpha = \mu U/T = 10^{-2}$. Then, by equation (18), the required value of ζ'' is 0·0992. From the plot of ζ' against ζ'' this corresponds to $\zeta' = 1{\cdot}075$, and by equation (17) $\theta = 28{\cdot}0°$. Table 1 gives a set of such calculations.

This method, with more intermediate values of $\mu U/T$, was used to plot figure 5. Also plotted on figure 5 are the experimental results, which are discussed in § 3.

2. Experiments

A systematic control of at least one of the relevant parameters, θ, $\mu U/\sigma$ or $T/\mu U$, was desirable for data correlation, but in fact could not be achieved easily in an experiment. A thin flexible sheet peeling at a small angle from a plane surface

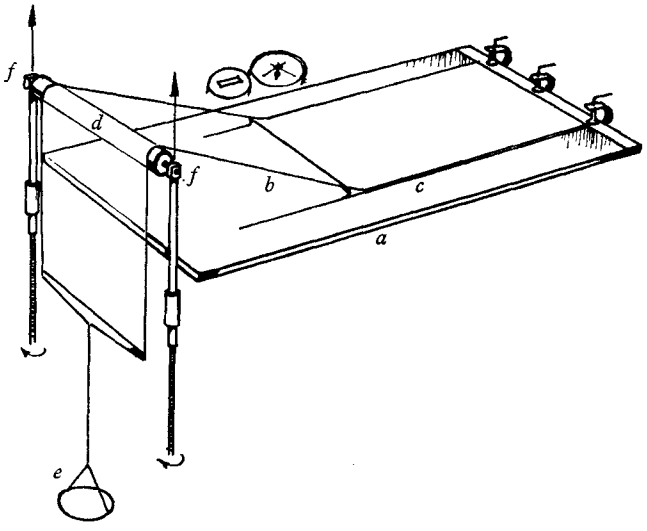

FIGURE 6. Experimental arrangement.

appears to be torsionally unstable when the peeling rate is a function of the applied force. Hence some form of lateral constraint was necessary. Furthermore, in order to avoid the conflicting limitations introduced by gravitational force and sheet stiffness, the plane surface had to be nearly horizontal.

The arrangement adopted, described below and sketched in figure 6, controlled none of the above variables directly, but permitted wide variations in them to be produced with ease, and enabled a steady state to be maintained for the major part of each test. It comprised a horizontal plate-glass surface (*a*) over which was laid a thin transparent plastic sheet, 30 cm in width and over 100 cm long (*b*).† A film of liquid (*c*) was sandwiched between the sheet and the glass surface. The sheet, of 'Melanex', approximately 4 μm thick, was clamped at one end to the

† For some tests at low peeling angles, a sheet 10·1 cm wide and 25 μm thick was used.

glass surface, and at the other end passed over a freely moving roller (*d*) the axis of which was parallel to the glass surface. The sheet at this end had attached along its edge a rigid metal strip, from which were suspended weights in a scale pan (*e*). The roller could be raised vertically at a constant pre-set rate by screws at the axle trunnion (*f*) driven by an infinitely variable speed drive. The rate of raising of the roller and the weight in the scale pan dictated the rate of peeling of the sheet from the glass, and the peeling angle. The peeling velocity and angle remained virtually constant for each run, except for the short starting period affected by inertia and the formation of a steady meniscus. A camera recorded time, meniscus position, and the counter which measured roller elevation.

Although precise control of liquid-film thickness was not theoretically necessary, the computation of corrections to the measured quantities required that it be known. Accordingly, films of uniform thickness were formed by use of a height-adjustable roller, manually operated, which was passed over the sheet as the liquid was being laid for each experimental run. For most tests the film was made 0·0025 cm thick, but variations in film thickness exerted no systematic effect upon the results.

Three liquids were used to form the adhesive layer; these were ethyl alcohol, castor oil, and a heavy lubricating oil, Shell 'Limea 81'. The viscosity of each of the oils was determined over a range of temperature by the falling-ball method, with appropriate corrections, and surface tension was found by the pendant drop method with Fordham's (1948) calculations, and by capillarity in a small tube. Alcohol properties were taken from physical tables. The range of properties so determined is listed below in table 2.

	μ poise	σ dyne/cm
Ethyl alcohol	0·0112–0·0126	21·6–22·7
Castor oil	7·8 –9·2	35·0–35·9
Limea 81 Oil	76·0 –100	33·6–36·0

TABLE 2

The experimental technique for all measurements was the same. The layer was rolled to the required thickness with the raising roller *d* at its lowest position. The requisite weights were placed in the scale pan and the variable-speed drive was pre-set at a chosen speed. A clutch was then engaged which simultaneously commenced to raise the roller *d* and to turn the counter. Sufficient photographs (between 3 and 6) were taken during the course of one run to provide at least two reducible results. Within each series of runs the drive speed was held more or less constant while the tension of the sheet was raised from run to run. The only parameter not directly determinable from the recorded results was θ, the peeling angle; this could be calculated approximately by trigonometry, but errors due to the weight of the liquid-laden strip and (in the tests at low $\mu U/\sigma$ and low θ) the thickness of the separating meniscus caused θ to be consistently underestimated. This first error could be accounted for by the correction

$$\Delta\theta = -wL/2T,$$

in which w is the loading per unit area on the strip and L is the peeled length. For the second error use is made of the observation that the height h is limited by gravity independently of $\mu U/\sigma$. For small peeling angles this height is

$$h_{\lim} = (4T/\rho g)^{\frac{1}{2}}$$

(where ρ is the liquid density), which for alcohol is 0·335 cm. Below this height the meniscus rises to h_0/m, being 0·0025 cm in most tests. As argued by Taylor (1963), gravity is unlikely to affect the value of m materially, but, to correct θ, h_0/m or $h_{\lim}$, whichever was the smaller, was subtracted from the recorded roller height.

3. Results and discussion

All the experimental results are plotted on figure 5, and are compared with their theoretical location. On this figure each experimental result is represented by its appropriate symbol, and the difference between its value, and the value of m it should possess as given by figure 2, is shown as a flag. Each flag terminates on a short line which represents the line of constant m to which it belongs. It is not possible to locate the point on this line because the source of the discrepancy could lie in any one of the three variables.

Symbols on figure 5 which have no flags are those for which the theoretical m-line coincides with the experimental points to within the radius of the symbol.

The number of symbols not possessing flags represents a large proportion of the total number of experiments, but before remarking on the quality of the agreement between theory and experiment it is desirable to see what a plot of this nature signifies.

When m is small, ζ is large, and the solutions of equation (6) corresponding to this large ζ are of the 'non-returning' variety. These solutions are characterized by a value of ζ'' which is nearly independent of ξ, so that the shape adopted by the peeling strip is parabolic:

$$\zeta = \tfrac{1}{2}c_0 x^2 + c_1 x + c_2,$$

from which

$$\zeta\zeta'' = \tfrac{1}{2}\zeta'^2 + c_0 c_2 - \tfrac{1}{2}c_1^2.$$

If the quadratic is a satisfactory fit to the exact solution above $\zeta = \zeta_1$, then $(\zeta - \zeta_1)\zeta_1'' = \frac{1}{2}(\zeta'^2 - \zeta_1'^2)$ for any greater value of ζ. Therefore, the solutions asymptote to

$$\zeta\zeta'' = \tfrac{1}{2}\zeta'^2. \tag{19}$$

In this case, by equations (11), (12), (16) and (17), the motion becomes independent of μU, and

$$\tan^2\theta = 4\sigma/T,$$

or for small peeling angles

$$\tan^2\tfrac{1}{2}\theta = \sigma/T. \tag{20}$$

But this equation is the same as that for the static balance between σ and T. This implies that, at low values of $\mu U/\sigma$, all experimental points will correspond to the theoretical lines regardless of the value of μU. The function for m assumed in figure 2 could be very much in error, but its influence upon the relationship between T and θ would be small.

It is noted that the disagreement between experiment and theory becomes more marked as m and θ increases. Discrepancies at high θ are to be expected because of the approximations contained in the analysis, but for those results below $\theta = 10°$, say, the disagreement probably arises largely from the inaccuracy of the assumed forms of F_1 and F_2.

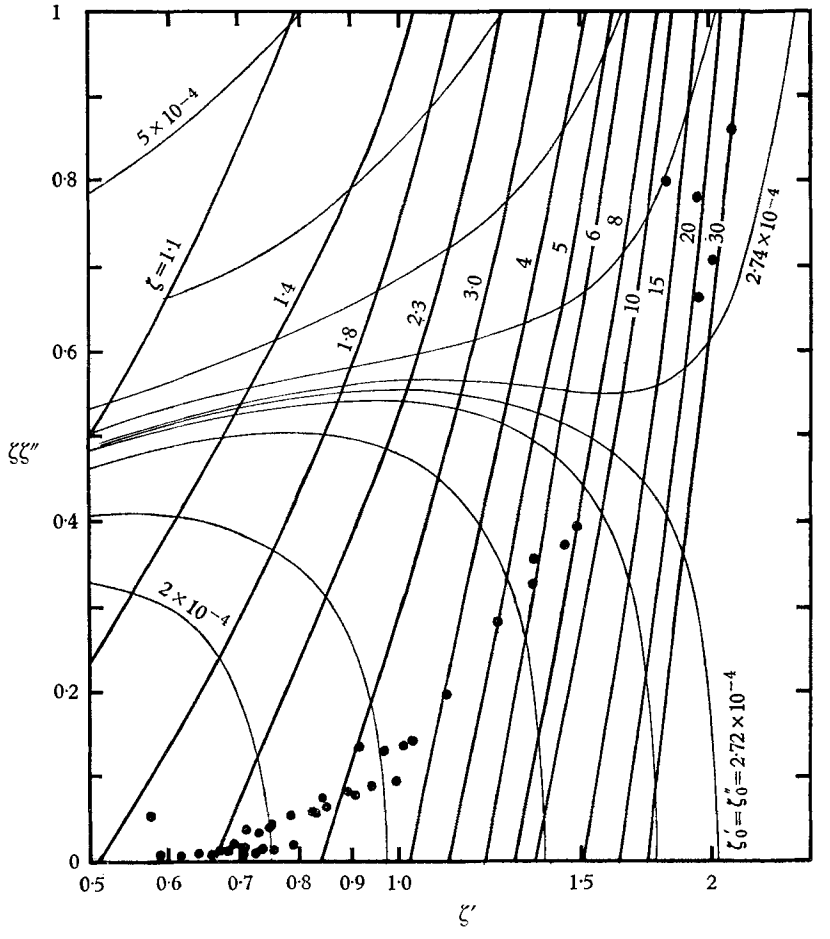

FIGURE 7. Determination of m from experiment.

With the computed solutions of equation (6) at hand it is possible to make an approximate estimate of F_1 at high values of $\mu U/\sigma$, from the experimental results. A plot is prepared of $\zeta\zeta''$ against ζ' and lines of constant ζ are marked upon it. Figure 7 shows part of such a plot. Now, if F_2 is assumed to be given by equation (14), and $F_1 = 1/\zeta$, then the experimental value of $\zeta\zeta''$ is given using equation (16). The experimental value of ζ' is calculated by equation (17), and each experimental point can be located upon figure 7. From this figure, ζ can be interpolated and the 'true' value of m calculated. It must be remembered, however, that F_2 has been *assumed* so that, quite apart from the crowding of ζ-lines at high ζ, errors must arise due to the inaccuracy of this function. Note that F_2 only appears

in $\zeta\zeta''$, and that the experimental value of this product is small as $\mu U/\sigma$ becomes of order unity (the experimental points group near the ζ'-axis). Therefore, the error in determining ζ is small for reasonably high values of $\mu U/\sigma$.

In figure 2 the experimental values of m, so determined, are compared with the assumed function. Only points for $\theta < 10°$ are plotted. At high $\mu U/\sigma$, the results seem to display asymptotic behaviour, but the asymptote is possibly somewhat greater than 0·4. F_1 is nevertheless a good approximation. At lower values of $\mu U/\sigma$ the scatter of results becomes more pronounced, because the experimental results become less and less sensitive to F_1. Within the limitations of the measured quantities, the agreement can be considered as quite acceptable.

4. Visual comparison with real adhesives in peeling

A characteristic feature of the meniscus formed when a viscous fluid separates between two diverging surfaces is the formation of 'webs' of fluid extending behind the leading edge of the meniscus 'fingers'. The appearance and form of these webs is observed to be dependent upon the angle of divergence of the surfaces and also upon $\mu U/\sigma$. Although their existence was known previously, Pearson's analysis (1960) to find the most unstable wavelength of lateral disturbances to the meniscus, and to relate it to experiments on spreading (one surface only in motion) of viscous liquids, was the first attempt at a rational description of the webs. Taylor (1963) publishes some photographs of webs produced in a similar physical situation, and Pitts & Greiller (1961) also comment on the ribbed appearance of liquid films rolled between the nip of adjacent counter-rotating cylinders. The same webbed appearance of the meniscus was noted in the present experiments on separation peeling. Figure 8 (plate 1) shows some typical examples of the form taken by the meniscus at values of $\mu U/\sigma$ corresponding with the approach of m to its asymptotic limit.

It is of interest to compare the present experimental observations with the appearance of the line of rupture in the peeling of ordinary commercially available impermeable pressure-sensitive tapes.

Figure 9 (plate 2) reproduces photographs of the meniscus formed using tape kindly provided by the Minnesota Mining and Manufacturing Co. Ltd., having what was described as an 'acrylate adhesive, adhesion level 30 units/in.' The two sticky surfaces were rolled together, care being taken wherever possible to avoid the trapping of air bubbles. They were then peeled apart in a small spring jig. In the first photograph, (I), peeling had just commenced and fingering is seen to be quite regular. The increase in peeling angle resulted in the shortening of the finger pattern (II). As the peeling progressed the meniscus approached small defects in the layer which resulted in the growth of cavities ahead of the fingers so that the regular pattern was lost (III). The occasional forking of webs is similar to that observed with the viscous-liquid experiments, and arises when the advancement of one air finger is inhibited by the more rapid advancement of the fingers adjacent to it. The behaviour is similar to that observed by Saffman & Taylor (1958) in a Hele–Shaw cell. As might be expected, the forking is inhibited by an increase in peeling angle.

Two other kinds of adhesive tape displayed a similar rupture-line behaviour: because of the superior uniformity of the adhesive layer, the former tape was preferred for photographic purposes.

Notwithstanding the apparent close similarity between the zone of rupture with Newtonian liquids and with practical adhesives, there is little ground for supposing that the real adhesives examined behave in all relevant respects as normal liquids. While some types of adhesive backing are known to exhibit an almost linear relationship between peeling rate and peeling force per unit width, which on the basis of the models presented would be reasonable evidence of 'Newtonian'-viscosity-dominated behaviour, such behaviour is the exception rather than the rule. Kaelble (1960) and Busse, Lambert & Verdery (1946), for example, give experimental results of peeling tests at high peeling angles in which some of the adhesives tested showed almost linear force/rate, but in most cases the relationship is found to approximate to a power one, of exponent greater than unity. However, such tests cannot be compared meaningfully with the present ones since they involve very high peeling angles, for which not only are the approximations of the present analysis no longer valid, but the effects of strip stiffness would almost certainly have influenced the results. Furthermore, these tests did not specifically distinguish the states in which the adhesive separated cleanly from one of the surfaces, and those in which the adhesive remained attached to both after rupture. The present analysis can justifiably be related only to the second case.

5. Concluding remarks

It appears that a Newtonian viscous adhesive layer, in peeling, can be described successfully by means of a simple Poiseuille model of behaviour, provided that the layer remains intact ahead of the line of rupture and that the peeling angle is small. The description relies upon a prediction of the significance of the parameter $\mu U/\sigma$ in defining the ratio of the thickness of the layer far upstream of rupture to the thickness at the rupture line. Within the experimental limitations, the prediction is confirmed, demonstrating that at low values of the peeling velocity U the relationship between peeling force T per unit width and peeling angle θ depends upon surface tension σ, but that a well-defined limiting relationship between $\mu U/\sigma$ and θ is approached; as σ becomes insignificant U is proportional to T for a given θ.

This result is analogous to the experimentally observed existence of an asymptotic limit to the proportion of liquid remaining after the evacuation of a two- or three-dimensional viscous-liquid-filled passage by a penetrating cavity or bubble, a situation which finds application in other cases of practical interest, as in cavitating lubrication and in applying surface coatings.

It is noted that the physical appearance of the zone of rupture of commercially available impermeable pressure-sensitive tapes in peeling is similar to that arising in the present experiments, provided that the adhesive remains attached to the tape and is unflawed ahead of the rupture line. The characteristic instability of the free surface gives rise to the formation of webs of adhesive separated by

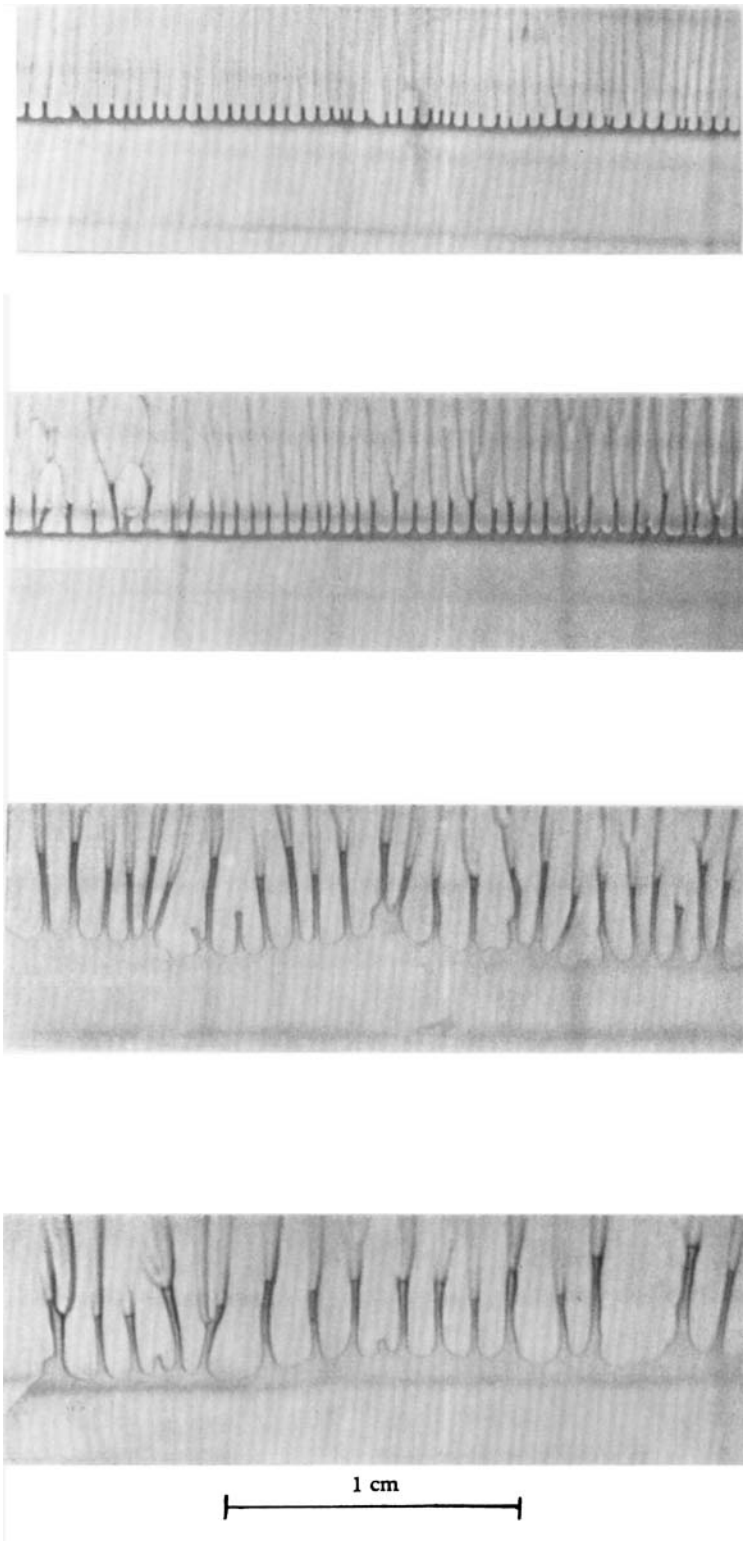

FIGURE 8. Meniscus appearance—viscous liquid. Peeling advances downwards.
$\mu = 73$ poise, $\sigma = 33{\cdot}6$ dyne/cm.

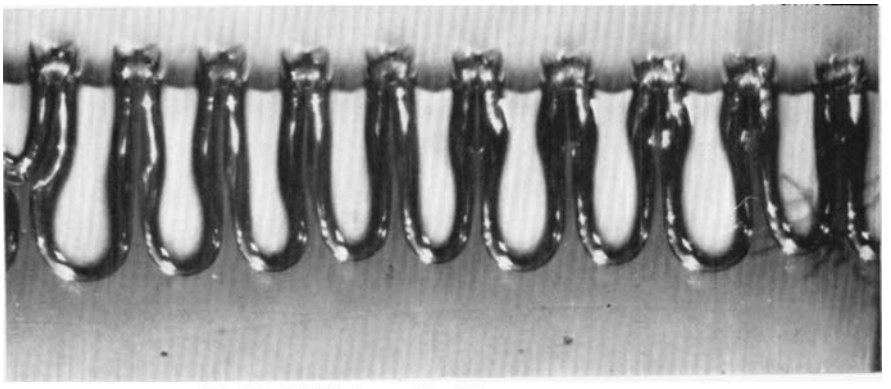

(I) $T = 0{\cdot}48$ kg/cm $2\theta = 38$

(II) $T = 0{\cdot}48$ kg/cm $2\theta = 55$

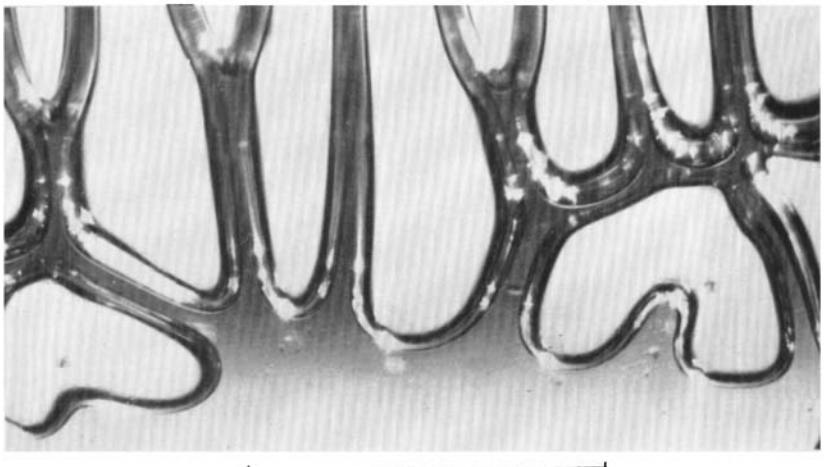

1 mm

(III) $T = 0{\cdot}87$ kg/cm $2\theta = 38$

FIGURE 9. Peeling of 'Acrylate' adhesive tape.
Peeling advances downwards.

penetrating air fingers. This similarity cannot however be considered as evidence of any detailed applicability of the present results to real adhesives in peeling.

One of us (A. D. McE.) expresses his gratitude for assistance given by an Australian C.S.I.R.O. Studentship and later by an Australian Public Service Board Scholarship.

REFERENCES

BICKERMANN, J. J. 1957 *J. Appl. Phys.* **28**, 1484.
BRETHERTON, F. P. 1961 *J. Fluid Mech.* **10**, 166.
BUSSE, W. F., LAMBERT, J. M. & VERDERY, R. B. 1946 *J. Appl. Phys.* **17**, 376.
CHANG, F. S. C. 1960 *Trans. Soc. Rheol.* **4**, 74.
COX, B. G. 1962 *J. Fluid Mech.* **14**, 81.
FAIRBROTHER, F. & STUBBS, A. E. 1935 *H. Chem. Soc.* **1**, 527.
FORDHAM, S. 1948 *Proc. Roy. Soc.* A, **194**, 1.
KAELBLE, D. H. 1960 *Trans. Soc. Rheol.* **4**, 45.
PEARSON, J. R. A. 1960 *J. Fluid Mech.* **7**, 481.
PITTS, E. & GREILLER, J. 1961 *J. Fluid Mech.* **11**, 33.
SAFFMAN, P. G. & TAYLOR, G. I. 1958 *Proc. Roy. Soc.* A, **245**, 312.
TAYLOR, G. I. 1961 *J. Fluid Mech.* **10**, 161.
TAYLOR, G. I. 1963 *J. Fluid Mech.* **16**, 595.